Journal of Innovative Optical Health Sciences
Vol. 6, No. 4 (2013) 1350033 (6 pages)

DOI: 10.1142/S1793545813500338

World Scientific
www.worldscientific.com



# PHOTOACOUSTIC VISCOELASTICITY IMAGING OF BIOLOGICAL TISSUES WITH INTENSITY-MODULATED CONTINUOUS-WAVE LASER

YUE ZHAO and SIHUA YANG*
*MOE Key Laboratory of Laser Life Science*
*and Institute of Laser Life Science*
*College of Biophotonics, South China Normal University*
*Guangzhou 510631, P. R. China*
**yangsh@scnu.edu.cn*

Received 4 June 2013
Accepted 22 July 2013
Published 28 August 2013

In this paper, a novel photoacoustic viscoelasticity imaging (PAVEI) technique that provides viscoelastic information of biological tissues is presented. We deduced the process of photoacoustic (PA) effect on the basis of thermal viscoelasticity theory and established the relationship between the PA phase delay and the viscoelasticity for soft solids. By detecting the phase delay of PA signal, the viscoelasticity distribution of absorbers can be mapped. Gelatin phantoms with different densities and different absorption coefficients were used to verify the dependence of PAVEI measurements. Moreover, tissue mimicking phantoms mixed with fat and collagen at different concentrations were used to testify the feasibility of this technique with reliable contrast. Finally, the PAVEI was successfully applied to discrimination between biological tissue constituents. Our experimental results demonstrate that this novel technique has the potential for visualizing the anatomical and biomechanical properties of biological tissues.

*Keywords*: Photoacoustic; phase delay; viscoelasticity; imaging.

## 1. Introduction

Viscoelastic property is an important physical-characterized parameter closely connected to the thermodynamic properties of materials, whose changes in biological tissues are often related to pathology.[1] For soft solid, such as cartilage, bone, tendon and muscle, they require viscoelastic information simultaneously to describe their mechanical behavior. Currently, a variety of morphological imaging techniques are investigated to detect the viscoelasticity of biological tissues. Intravascular ultrasound elastography, combined with the pressure measurement, allows the detection of the viscoelasticity of atherosclerotic lesions.[2] An optical method, Laser Speckle Imaging, that has been described measures the Brownian motion of plaque molecules to provide the viscoelasticity of biological

tissues.[3] However, these techniques still suffer from low resolution and low contrast in detecting applications.[4] Therefore, a detection technique to characterize viscoelasticity of tissues with higher sensitivity and higher resolution would be of great progress in medical application and clinical research.

Photoacoustic (PA) imaging is a hybrid imaging modality, based upon the use of laser-generated ultrasound, which combines the high optical contrast with the high spatial resolution of ultrasound.[5–9] In the past decade, PA imaging has made great progress in biomedical application, such as tumor detection,[10,11] noninvasive monitoring of vasculature networks[12,13] and blood oxygen saturation,[14] brain functional imaging[15–17] and identification of atherosclerotic plaques.[18] PA effect refers to the generation of acoustic wave by the absorption of laser. By reason of the viscoelasticity of tissue, there is a phase delay when PA wave launches from the thermal expansion source caused by the excitation laser. Different tissue types or pathology with corresponding viscoelastic properties will lead to different phase delay of PA wave. Therefore, photoacoustic viscoelasticity imaging (PAVEI) can be obtained based on the contrast with phase delay.

In this paper, we deduced the process of PA effect on the basis of thermal viscoelasticity theory and established the relationship between the PA phase delay and the viscoelasticity for soft solids. Moreover, a PAVEI system was developed and gelatin phantoms were used to testify the feasibility of this technique with reliable contrast. Finally, the PAVEI was successfully applied to the discrimination between biological tissue constituents.

## 2. Methods and Materials

### 2.1. *Principle of the PAVEI*

Intensity-modulated continuous-wave (CW) laser was used to radiate absorptive isotropic viscoelastic structures, and the light intensity is given by $I = 1/2\ I_0(1 + \cos\omega t)$, where $I_0$ is the time-averaged light intensity, and $\omega$ is the modulation frequency. Light absorption by the absorber results in a sinusoidal temperature variation in the form of $T = T_0 e^{i\omega t}$ due to the nonradiative transition, and then causes thermal expansion and shrink as well as PA wave generation based on the thermoelastic mechanism.[19] In the above process, the cyclical heating in local region induces the thermal stress, and the strain generates due to the stress in the form of the force-produced PA waves. Because of the damping effect due to the viscoelasticity of biological tissues, it could be found that the strain also alternated periodically but would be out of phase with the stress.

In fact, the above-mentioned process is a problem of the rheonomous thermal stress caused by a periodically variational point heat source for unbounded isotropic viscoelastic solid. By resolving this problem, the radial thermal stress in the spherical coordinate system can be expressed as[20]:

$$\sigma = -\frac{4G}{r}\frac{\partial\Phi}{\partial r} + \rho\frac{\partial^2\Phi}{\partial t^2}, \tag{1}$$

where $G$ is the Green Function of thermal conduction; $\Phi$ is the thermoelastic displacement potential and defined by $\Delta\Phi = \alpha T(1+\nu)/(1-\nu)$; $\alpha$ is the coefficient of linear expansion; $\nu$ is the Poisson ratio. In the condition of temperature $T = T_0 e^{i\omega t}$, the stress $\sigma$ can be rewritten as[21]:

$$\sigma = -E\alpha T_0 e^{i\omega t}/(1-\nu), \tag{2}$$

where $E$ is the Young's modulus, $\omega$ is the modulation frequency. In rheological Kelvin–Voigt model, the constitutive equation in terms of a stress–strain relationship can be expressed as[22]:

$$\sigma = E\varepsilon + \eta\dot{\varepsilon}. \tag{3}$$

Combining the Eqs. (2) and (3), we have:

$$\varepsilon(t) = \varepsilon_A e^{i(\omega t+\delta)} \tag{4}$$

$$\delta = \arctan\frac{\eta\omega}{E}, \tag{5}$$

where $\varepsilon_A = (-E^2\alpha T)/[(E^2+\eta^2\omega^2)\cos\delta(1-\nu)]$ is the amplitude of complex strain. The physical significance of Eq. (4) indicates that $\delta$ is the phase delay of the strain response to the stress. From Eq. (5), we can know the relationship between phase delay $\delta$ and the viscosity–elasticity ratio $\eta/E$.

### 2.2. *Instrumentation of the PAVEI*

The experimental schematic diagram is shown in Fig. 1(a). A CW laser with wavelength of 808 nm was used as excitation source. The intensity of CW laser was modulated by the electro-optic light modulator with a 90% modulation depth at frequency of 50 kHz. The modulation signal applied to

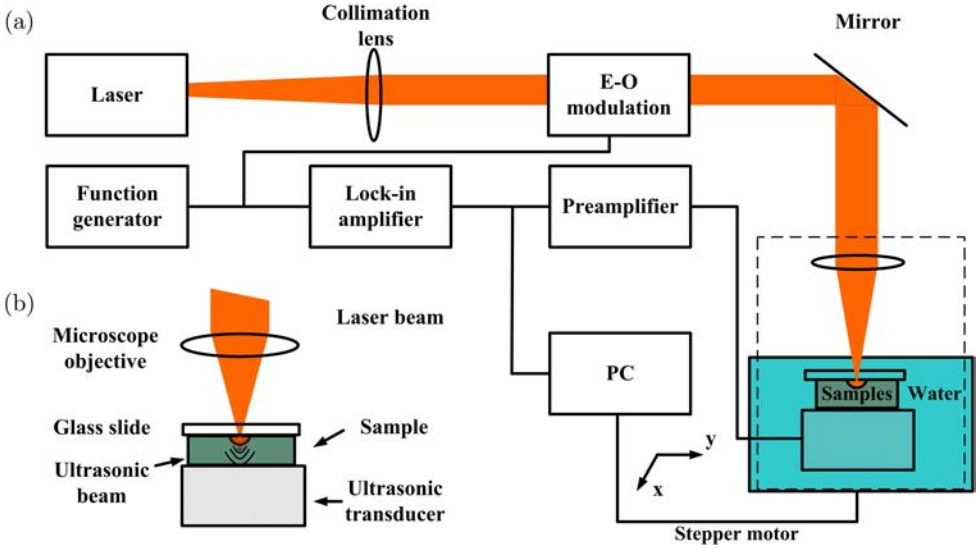


Fig. 1. (a) Scheme of experimental setup for PAVEI. (b) The specific structure indicated by the dashed line.

the voltage amplifier attached to the modulator from function generator was equal to the center frequency of the ultrasonic transducer. The center frequency of the ultrasonic transducer is also 50 kHZ which is equal to the modulation signal. And the diameter of the transducer is about 6 cm. A lock-in amplifier was used to detect the dominant frequency of PA wave and calculate the phase lag between the dominant frequency PA wave and the reference signal. Samples were made into slices with the thickness of 0.3 mm. Laser through an optical lens illuminated the target at focal point of about 0.1 mm. The laser power density on the sample surface was limited to 200 mW/cm$^2$. The transducer was placed against the laser and fastened to a 2D scan platform which moved point by point. As shown in Fig. 1(b), the sample and the transducer were fixed together, and the distance from light spot to the transducer was kept consistent strictly when the sample was changed.

## 3. Results

### 3.1. *PAVEI of gelatin phantoms*

Gelatin phantoms with different absorption coefficients but the same density were controlled by the interfusing of ink with a proportion of 2% and 4%, respectively. According to the results shown in Fig. 2, the measured PA phase delays are almost the same in every density, which indicates that the absorption coefficient has little impact on PA phase delay which was mainly determined by the different viscoelastic properties.

In order to testify the feasibility of this technique with reliable contrast, three gelatin phantoms with different densities of 1%, 5% and 1% were used to simulate tissues with different viscoelastic properties. Figure 3(a) shows the photograph of the gelatin phantoms with different density. All samples were clearly observed in the PAVEI image as shown in Fig. 3(b). Figure 3(c) is the reconstruction profiles of PAVEI image at the position indicated by dashed lines. As predicted theoretically, the observed phase delay between the dominant frequency of PA wave and the modulation signal increased with the increase in density of sample.

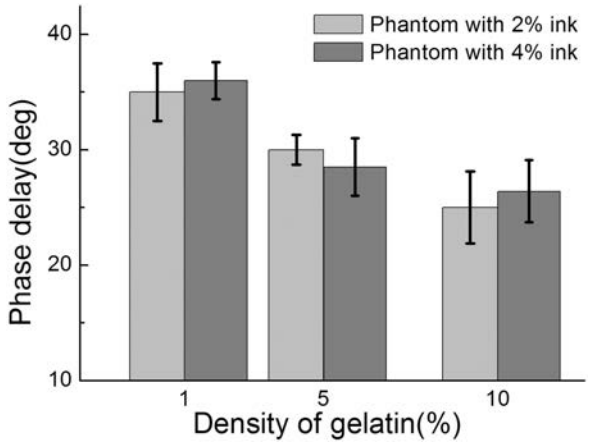


Fig. 2. Phase delay obtained by PAVEI from gelatin with different absorption coefficients.

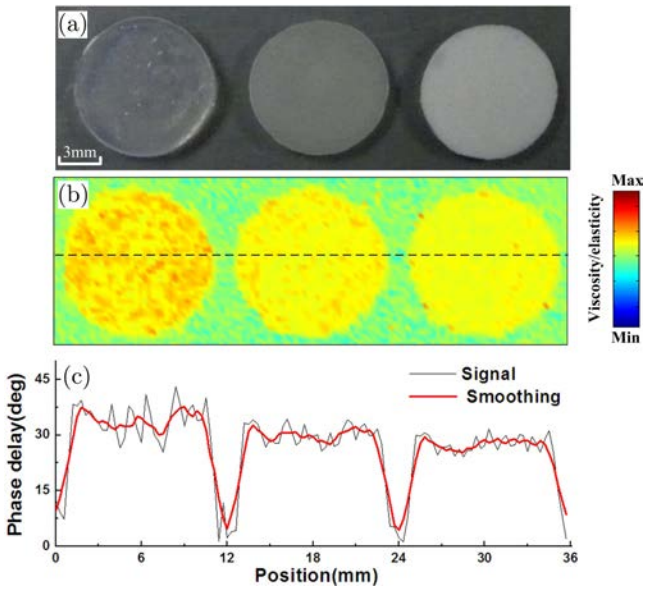


Fig. 3. (a) Photograph of the gelatin phantoms with the gelatin density of 1%, 5% and 10%, respectively. (b) The PAVEI of gelatin phantoms with different viscoelastic properties. (c) Reconstruction profiles of PAVEI image at the position indicated by dashed lines.

### 3.2. *PAVEI of tissue-mimicking phantom*

To test and verify the relation between features associated with biological tissues, a representative result from the experiments using tissue-mimicking phantom is shown in Fig. 4. Two components (fat and collagen) were mixed with the gelatin with different concentrations to simulate biological tissues. Figure 4(a) is the photograph of the phantoms prepared by mixing gelatin with fat and collagen at different concentrations of 30%, 60% and 90%, respectively. All targets are clearly shown in the PAVEI images in Fig. 4(b) and matched well with the photograph. The phase delay of PA signals are quantified as a function of the mechanical properties of the phantoms. Figures 4(c) and 4(d) show the reconstruction profiles of PAVEI image at the position indicated by red and blue lines. As predicted theoretically, the observed phase delay of the PA signals increased well with the increase in density of the fat in contrast to collagen.

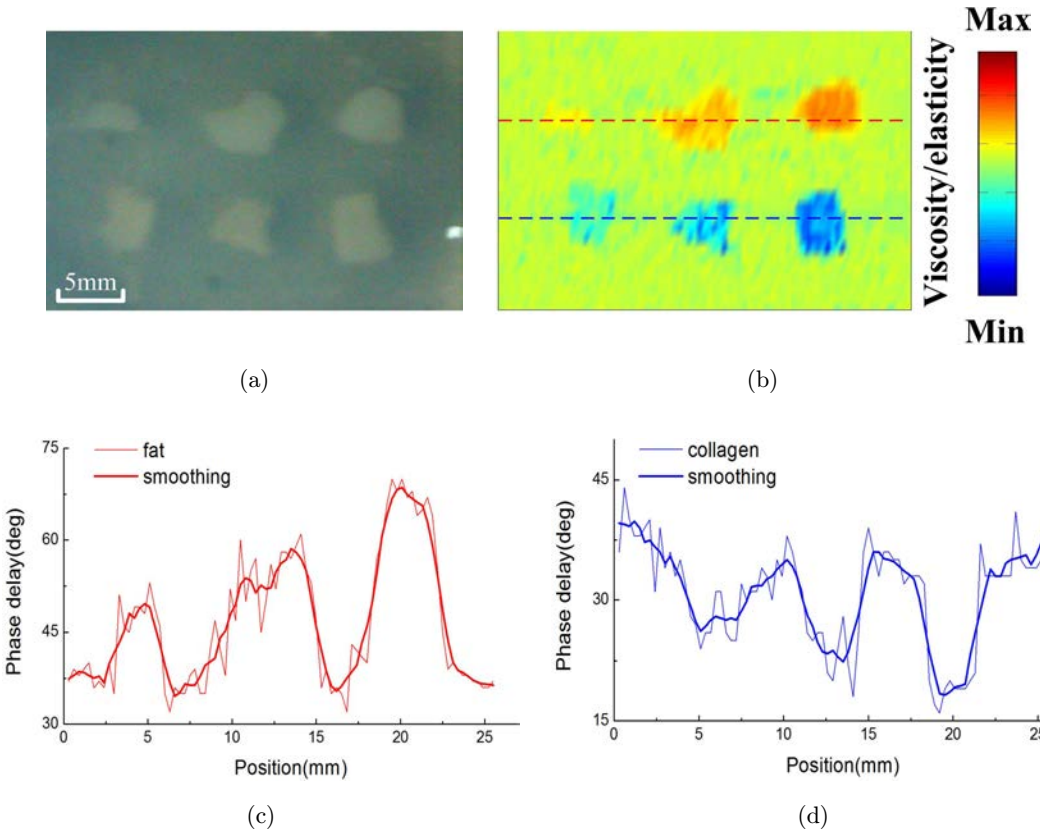


Fig. 4. (a) Photograph of the phantoms prepared by mixing gelatin with fat and collegen at different concentrations. (b) The PAVEI of gelatin phantoms. (c) and (d) Reconstruction profiles of PAVEI image at the position indicated by red and blue lines.

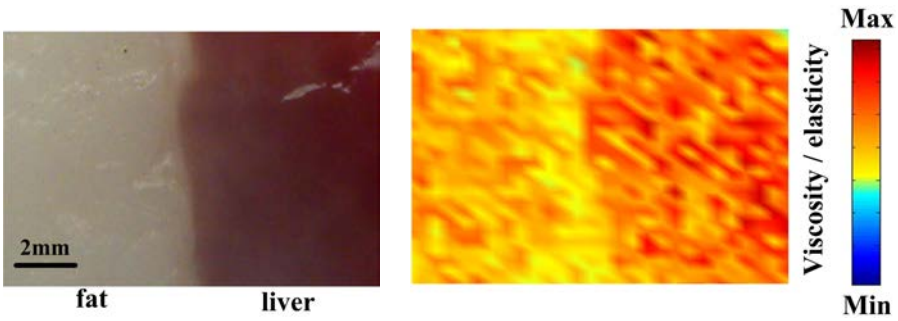


(a) (b)

Fig. 5. (a) Photograph of biological tissues (fat and liver). (b) Viscoelasticity distribution of the sample detected by PAVEI.

### 3.3. *PAVEI of biological samples*

To verify the feasibility of PAVEI of tissues, two biological samples (fat and liver of pig) were tested as the method shown in Fig. 5. The imaging sample and the scanning area were shown in Fig. 5(a). PA phase delay measured from each scanning point was projected to image the relative viscoelasticity distribution. The reconstruction image is shown in Fig. 5(b), and the color bar represents the relative viscosity–elasticity ratio. Multiple studies have shown that the liver tissue had higher viscosity–elasticity ratio than fat, in which variation tendency was also matched well with the data measured by PAVEI. Our results clearly revealed the boundary of the composite sample and the imaging intensity for distinguishing different tissues. Overall, the PAVEI was successfully applied to the discrimination between biological tissue constituents and this novel technique can be used to characterize the biomechanical property of biological tissues.

## 4. Discussion

The accuracy of the measurement system was limited by the time constant of the lock-in amplifier and the signal-to-noise ratio (SNR). A longer time constant will improve the performance, but reduce the scanning speed and SNR. A value of 30 ms time constant is selected to perform experiments, which is the main reason to cause the uneven distribution of the pixel values in Fig. 3. Use of a differential preamplifier can potentially improve the SNR.

This PAVEI system works only in transmission mode. In this model, the velocities of different samples will lead to different phase error, which affect the accurate measurement of samples. This limits its applications in the clinic. In the future, an acoustic-optical confocal mode would be adopted to increase the SNR. This reflection mode with illumination and ultrasonic detection from the same side will be necessary to avoid the phase error resulting from the ultrasound path difference, which is convenient to realize the measurement *in vivo*.

All experiments were performed in a water tank at room temperature (23°C). It is possible that changes in temperature can change the characteristics of the samples. Hence, the influence of temperature changes on mechanical properties of the tissues will be investigated. Meanwhile, precise measurements of phase delay from *ex vivo* tissues may slightly vary under *in vivo* conditions. However, in the present study, due to the different phase delay values between different tissues, it can be anticipated that these relative differences will be maintained under *in vivo* conditions.

## 5. Conclusion

In summary, we have proposed a novel technique for characterization of the biological tissue viscoelasticity with PAVEI. The theoretical approach of the process of PA effect on the basis of thermal stress problem was deduced to explain the PA phase delay phenomenon. This technique has not only higher sensitivity but also higher resolution in viscoelasticity measurements. The high contrast result reflecting the tissue viscoelasticity information with PAVEI was successfully achieved. Diagnostic detection of atherosclerotic plaque and skin tumor would be the most potential applications of this technique, which are sensitive to the viscoelastic properties of tissue. It is trusted that PAVEI would have great potential application in both biomedical research and clinical study.

## Acknowledgments

This research is supported by the National Basic Research Program of China (2011CB910402; 2010CB732602), the Program for Changjiang Scholars and Innovative Research Team in University (IRT0829), the National Natural Science Foundation of China (81127004, 11104087), and the Foundation for Distinguished Young Talents in Higher Education of Guangdong, China (LYM10061), the Specialized Research Fund for the Doctoral Program of Higher Education (20114407120001), and the Science and Technology Project of Guangzhou, China (2012J4100114).

## References

1. J. D. Ferry, H. S. Myers, "*Viscoelastic Properties of Polymers*," Wiley, Newyork (1980).
2. B. Heintz, D. J. Vom, K. Roeber, A. Doettger, P. Hanrath, H. G. Sieberth, "Effects of blood pressure reduction on the elastic profile of the aortic tree in patients with coronary heart disease," *Am. J. Hypertens.* **8**, 584–590 (1995).
3. S. K. Nadkarni, B. E. Bouma, T. Helg, R. Chan, E. Halpern, A. Chau, M. S. Minsky, J. T. Motz, S. L. Houser, G. J. Tearney, "Characterization of atherosclerotic plaques by laser speckle imaging," *Circulation* **112**, 885–892 (2005).
4. I. K. Jang, B. E. Bouma, D. H. Kang, S. J. Park, S. W. Park, K. B. Seung, K. B. Choi, M. Shishkov, K. Schlendorf, E. Pomerantsev, S. L. Houser, H. T. Aretz, G. J. Tearney, "Visualization of coronary atherosclerotic plaques in patients using optical coherence tomography: Comparison with intravascular ultrasound," *J. Am. Coll. Cardiol.* **39**, 604–609 (2002).
5. D. Yang, D. Xing, H. Gu, Y. Tan, L. Zeng, "Fast multielement phase-controlled photoacoustic imaging based on limited-field-filtered back-projection algorithm," *Appl. Phys. Lett.* **87**, 194101 (2005).
6. Y. Wang, D. Xing, Y. Zeng, "Photoacoustic imaging with deconvolution algorithm," *Phys. Med. Biol.* **49**, 3117 (2004).
7. C. Lou, S. Yang, Z. Ji, Q. Chen, D. Xing, "Ultrashort microwave-induced thermoacoustic imaging: A breakthrough in excitation efficiency and spatial resolution," *Phys. Rev. Lett.* **109**, 218101 (2012).
8. T. Jetzfellner, V. Ntziachristos, "Performance of blind deconvolution in optoacoustic tomography," *J. Innov. Opt. Health Sci.* **4**, 385–393 (2011).
9. N. S. Eikje, "Potential of *in vivo* latent-time estimation by laser and optical techniques in clinical and experimental dermatology," *J. Innov. Opt. Health Sci.* **4**, 421–428 (2011).
10. Y. Q. Lao, D. Xing, S. H. Yang, L. Z. Xiang, "Noninvasive photoacoustic imaging of the developing vasculature during early tumor growth," *Phys. Med. Biol.* **53**, 4203–4212 (2008).
11. B. Yin, D. Xing, Y. Wang, Y. Zeng, Y. Tan, Q. Chen, "Fast photoacoustic imaging system based on 320-element linear transducer array," *Phys. Med. Biol.* **49**, 1339 (2004).
12. H. F. Zhang, K. Maslov, M. L. Li, G. Stoica, L. H. V. Wang, "*In vivo* volumetric imaging of subcutaneous microvasculature by photoacoustic microscopy," *Opt. Express* **14**, 9317–9323 (2006).
13. S. Yang, D. Xing, Q. Zhou, "Functional imaging of cerebrovascular activities in small animals using high-resolution photoacoustic tomography," *Med. Phys.* **34**, 3294 (2007).
14. G. Yin, D. Xing, S. Yang, "Dynamic monitoring of blood oxygen saturation *in vivo* using double-ring photoacoustic sensor," *J. Appl. Phys.* **106**, 013109 (2009).
15. S. H. Yang, D. Xing, Y. Q. Lao, D. W. Yang, L. M. Zeng, L. Z. Xiang, W. R. Chen, "Noninvasive monitoring of traumatic brain injury and post-traumatic rehabilitation with laser-induced photoacoustic imaging," *Appl. Phys. Lett.* **90**, 243902 (2007).
16. Y. G. Zeng, D. Xing, Y. Wang, B. Z. Yin, Q. Chen, "Photoacoustic and ultrasonic coimage with a linear transducer array," *Opt. Lett.* **29**, 1760–1762 (2004).
17. Z. Luo, C. Du, "Power of dual-wavelength approaches in studying physiological and functional changes of intact heart and *in vivo* brain," *J. Innov. Opt. Health Sci.* **4**, 261–268 (2011).
18. B. Wang, E. Yantsen, T. Larson, A. B. Karpiouk, S. Sethuraman, J. L. Su, K. Sokolov, S. Y. Emelianov, "Plasmonic intravascular photoacoustic imaging for detection of macrophages in atherosclerotic plaques," *Nano Lett.* **9**, 2212–2217 (2009).
19. C. Lou, D. Xing, "Photoacoustic measurement of liquid viscosity," *Appl. Phys. Lett.* **96**, 211102 (2010).
20. Y. Takeuchi, "*Thermal Stress*", Science Press (1978).
21. A. F. Mak, W. M. Lai, V. C. Mow, "Viscoelastic properties of proteoglycan subunits and aggregates in varying solution concentrations," *J. Biomech.* **20**, 703–714 (1987).
22. H. A. Baraes, J. F. Hutton, K. Walters, "*An Introduction to Rheology*," Elsevier (1989).